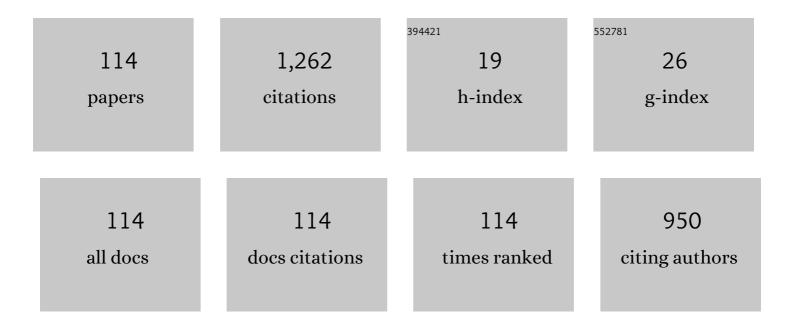
Jack J Yoh

List of Publications by Year in descending order

Source: https://exaly.com/author-pdf/5087601/publications.pdf Version: 2024-02-01



#	Article	IF	CITATIONS
1	Thermal decomposition behaviour and chemical kinetics of tungsten based electrically controlled solid propellants. Combustion and Flame, 2022, 238, 111752.	5.2	8
2	Accurate real-time monitoring of fine dust using a densely connected convolutional networks with measured plasma emissions. Chemosphere, 2022, 293, 133604.	8.2	5
3	Observation of gunpowder-like thermochemical responses of a thermal energy storage system based on KNO3/NaNO3/Graphite exposed to a heat transfer fluid. Applied Thermal Engineering, 2022, 207, 118215.	6.0	4
4	Development of a compact all-in-one chemical sensing module for in situ detection of fine dust components based on spark-induced plasma spectroscopy. Measurement: Journal of the International Measurement Confederation, 2022, 192, 110860.	5.0	3
5	Ignition and combustion behavior of zirconium-based pyrotechnic igniters and pyrotechnic delays under aging. Proceedings of the Combustion Institute, 2021, 38, 4373-4381.	3.9	7
6	Insights into aging mechanism of Ti-metal based pyrotechnics and changes in thermo-kinetic characteristics. Proceedings of the Combustion Institute, 2021, 38, 4441-4449.	3.9	7
7	Electronegative microchannel guided streamer propagation for in-liquid spark breakdown applications. Applied Physics Letters, 2021, 118, .	3.3	6
8	Burning Characteristics of Pyrotechnic Time-Delay Composition Subjected to Moisture and Heat. Journal of Propulsion and Power, 2021, 37, 868-875.	2.2	1
9	Onsite real-time detection of covid-like-virus transmission through air using spark-induced plasma spectroscopy. Science of the Total Environment, 2021, 770, 144725.	8.0	4
10	Investigation of aging induced processes on thermo-kinetic and combustion characteristics of tungsten pyrotechnic delay composition. Combustion and Flame, 2021, 228, 114-127.	5.2	14
11	A liquid breakdown driven non-invasive microjet injection system. Medical Engineering and Physics, 2021, 92, 54-63.	1.7	3
12	Addressing the complex geometric effects on the three-dimensional transition to detonation in hydrocarbon-air mixtures using a parametrized level-setÂalgorithm. International Journal of Hydrogen Energy, 2021, 46, 27827-27840.	7.1	0
13	A reactive hydrodynamic simulation of noise propagation for a concrete-confined detonation. AIP Advances, 2021, 11, 085009.	1.3	0
14	Understanding the effects of blast loads on open spaces and enclosed structures in simulations and experiments. Shock Waves, 2020, 30, 843-854.	1.9	2
15	Critical changes in the ignition and combustion characteristics of aged titanium-based initiators. Combustion and Flame, 2020, 221, 74-85.	5.2	9
16	Understanding the effects of hygrothermal aging on thermo-chemical behaviour of Zr-Ni based pyrotechnic delay composition. Fuel, 2020, 281, 118776.	6.4	10
17	On a New Correlation between Reaction Mechanism and the Ignition Delay Time for Titanium-based Pyrotechnic Initiators Exposed to Various Aging Conditions. , 2020, , .		Ο
18	Multiscale modeling of transients in the shock-induced detonation of heterogeneous energetic solid fuels. Combustion and Flame, 2020, 221, 401-415.	5.2	9

#	Article	IF	CITATIONS
19	Real-time monitoring of toxic components from fine dust air pollutant samples by utilizing spark-induced plasma spectroscopy. Chemosphere, 2020, 257, 127237.	8.2	12
20	A numerical investigation of the effects of hydrogen addition on combustion instability inside a partially-premixed swirl combustor. Applied Thermal Engineering, 2020, 176, 115478.	6.0	24
21	An optimal configuration for spark-induced breakdown spectroscopy of bulk minerals aimed at planetary analysis. Journal of Analytical Atomic Spectrometry, 2020, 35, 1103-1114.	3.0	13
22	Chemical kinetics of multi-component pyrotechnics and mechanistic deconvolution of variable activation energy. Proceedings of the Combustion Institute, 2019, 37, 3193-3201.	3.9	5
23	Towards understanding the effects of heat and humidity on ageing of a NASA standard pyrotechnic igniter. Scientific Reports, 2019, 9, 10203.	3.3	21
24	A non-calorimetric approach for investigating the moisture-induced ageing of a pyrotechnic delay material using spectroscopies. Scientific Reports, 2019, 9, 15228.	3.3	8
25	Modeling the shock-induced multiple reactions in a random bed of metallic granules in an energetic material. Combustion and Flame, 2019, 210, 54-70.	5.2	12
26	Thermochemical characterization of Zr/Fe2O3 pyrotechnic mixture under natural aging conditions. Journal of Applied Physics, 2019, 126, .	2.5	8
27	Slow and rapid thermal decomposition characteristics of enhanced blast explosives for burning in fuel-rich, oxygen-rich conditions. Thermochimica Acta, 2019, 678, 178300.	2.7	10
28	Double-pulse laser synchronization aimed at simultaneous detection of enhanced atomic and molecular signals at low pressure conditions. Spectrochimica Acta, Part B: Atomic Spectroscopy, 2019, 157, 12-21.	2.9	9
29	Numerical analysis of the effect of the hydrogen composition on a partially premixed gas turbine combustor. International Journal of Hydrogen Energy, 2019, 44, 6278-6286.	7.1	16
30	Parametric study of a VLS based on 2-D FSI analysis. Aerospace Science and Technology, 2019, 84, 530-542.	4.8	0
31	Two-dimensional measurement of hydrocarbon fuel concentration using multiple laser-induced plasma-forming regions. Optics Express, 2019, 27, 5144.	3.4	6
32	Novel utilization of the molecular band signal in metal oxides: understanding the aging process of pyrotechnic substances by using laser induced plasma emissions. Optical Materials Express, 2019, 9, 410.	3.0	12
33	Development and Application of Constant Flow Generating Injector with Pulse Energy Source as Driving Force. Journal of the Korean Society for Precision Engineering, 2019, 36, 497-503.	0.2	0
34	A two-phase model for aluminized explosives on the ballistic and brisance performance. Journal of Applied Physics, 2018, 123, .	2.5	9
35	Analytical Methods to Distinguish the Positive and Negative Spectra of Mineral and Environmental Elements Using Deep Ablation Laser-Induced Breakdown Spectroscopy (LIBS). Applied Spectroscopy, 2018, 72, 896-907.	2.2	4
36	Formation of double front detonations of a condensed-phase explosive with powdered aluminium. Combustion Theory and Modelling, 2018, 22, 378-393.	1.9	5

#	Article	IF	CITATIONS
37	Reconstruction of chemical fingerprints from an individual's time-delayed, overlapped fingerprints via laser-induced breakdown spectrometry (LIBS) and Raman spectroscopy. Microchemical Journal, 2018, 139, 386-393.	4.5	15
38	Forensic Discrimination of Latent Fingerprints Using Laser-Induced Breakdown Spectroscopy (LIBS) and Chemometric Approaches. Applied Spectroscopy, 2018, 72, 1047-1056.	2.2	16
39	Toward understanding the aging effect of energetic materials via advanced isoconversional decomposition kinetics. Journal of Thermal Analysis and Calorimetry, 2018, 133, 737-744.	3.6	16
40	A reduced order model for prediction of the burning rates of multicomponent pyrotechnic propellants. Applied Thermal Engineering, 2018, 130, 492-500.	6.0	8
41	A multi-scale simulation of hot spot initiation of detonation utilizing experimental measurements. AIP Advances, 2018, 8, 105217.	1.3	6
42	A reactive flow simulation for the anisotropic ignition of an explosive crystal using adaptive mesh refinement. Journal of Applied Physics, 2018, 124, 145903.	2.5	2
43	Modeling the effects of aluminum and ammonium perchlorate addition on the detonation of the high explosives C4H8O8N8 (HMX) and C3H6O6N6 (RDX). Journal of Applied Physics, 2018, 124, .	2.5	5
44	The hygrothermal aging effects of titanium hydride potassium perchlorate for pyrotechnic combustion. Thermochimica Acta, 2018, 665, 102-110.	2.7	9
45	Numerical Simulation of Fluid–Structure Interaction Problem Associated with Vertical Launching System. Journal of Spacecraft and Rockets, 2018, 55, 948-958.	1.9	3
46	Towards simplified monitoring of instantaneous fuel concentration in both liquid and gas fueled flames using a combustor injectable LIBS plug. Energy, 2018, 160, 225-232.	8.8	11
47	Kinetics deconvolution study of multi-component pyrotechnics. Thermochimica Acta, 2018, 667, 27-34.	2.7	16
48	lgnition sensitivity study of an energetic train configuration using experiments and simulation. Journal of Applied Physics, 2018, 123, 225901.	2.5	0
49	Accuracy Enhancement of Raman Spectroscopy Using Complementary Laser-Induced Breakdown Spectroscopy (LIBS) with Geologically Mixed Samples. Applied Spectroscopy, 2017, 71, 678-685.	2.2	10
50	Geometrically nonlinear quadratic solid/solidâ€shell element based on consistent corotational approach for structural analysis under prescribed motion. International Journal for Numerical Methods in Engineering, 2017, 112, 434-458.	2.8	14
51	Characterization of display pyrotechnic propellants: Burning rate. Applied Thermal Engineering, 2017, 121, 761-767.	6.0	11
52	Towards reconstruction of overlapping fingerprints using plasma spectroscopy. Spectrochimica Acta, Part B: Atomic Spectroscopy, 2017, 134, 25-32.	2.9	14
53	A full-scale hydrodynamic simulation of energetic component system. Computers and Fluids, 2017, 156, 368-383.	2.5	10
54	Performance characterization of a miniaturized exploding foil initiator via modified VISAR interferometer and shock wave analysis. Journal of Applied Physics, 2017, 121, .	2.5	12

#	Article	IF	CITATIONS
55	Shock to detonation transition analysis using experiments and models. Proceedings of the Combustion Institute, 2017, 36, 2699-2707.	3.9	4
56	All Eulerian method of computing elastic response of explosively pressurised metal tube. Combustion Theory and Modelling, 2017, 21, 293-308.	1.9	4
57	Skin preâ€eblation and laser assisted microjet injection for deep tissue penetration. Lasers in Surgery and Medicine, 2017, 49, 387-394.	2.1	7
58	Characterization of display pyrotechnic propellants: Colored light. Applied Thermal Engineering, 2017, 110, 1066-1074.	6.0	14
59	A check valve controlled laser-induced microjet for uniform transdermal drug delivery. AIP Advances, 2017, 7, 125206.	1.3	5
60	Simulating sympathetic detonation using the hydrodynamic models and constitutive equations. Journal of Mechanical Science and Technology, 2016, 30, 5491-5502.	1.5	7
61	Numerical Investigation of Kerosene-Based Pulse-Detonation Loading on the Metal Tubes. Journal of Propulsion and Power, 2016, 32, 1146-1152.	2.2	1
62	Advancing the experimental design for simultaneous acquisition of laser induced plasma and Raman signals using a single pulse. Spectrochimica Acta, Part B: Atomic Spectroscopy, 2016, 123, 1-5.	2.9	14
63	Standoff Detection of Geological Samples of Metal, Rock, and Soil at Low Pressures Using Laser-Induced Breakdown Spectroscopy. Applied Spectroscopy, 2016, 70, 1411-1419.	2.2	30
64	Analysis on shock attenuation in gap test configuration for characterizing energetic materials. Journal of Applied Physics, 2016, 119, 145902.	2.5	10
65	Isoconversional Method for Extracting Reaction Kinetics of Aluminized Cyclotrimethylene-Trinitramine for Propulsion. Journal of Propulsion and Power, 2016, 32, 777-784.	2.2	7
66	Synchronization of skin ablation and microjet injection for an effective transdermal drug delivery. Applied Physics A: Materials Science and Processing, 2016, 122, 1.	2.3	7
67	Simultaneous optical ignition and spectroscopy of a two-phase spray flame. Combustion and Flame, 2016, 165, 334-345.	5.2	23
68	On the elasto-plastic response of combustion tube subjected to kerosene-air detonation loading. , 2015, , .		0
69	A direction sensitive detonation model for granular to continuum scale for shock initiation of pentaerythritol tetranitrate single crystal in multi-dimensions. AIP Advances, 2015, 5, .	1.3	2
70	A detailed numerical calibration of shock pressure in the gap test configuration for characterizing non-ideal energetic materials. , 2015, , .		1
71	The application of magnetic field at low pressure for optimal laser-induced plasma spectroscopy. Spectrochimica Acta, Part B: Atomic Spectroscopy, 2015, 110, 7-12.	2.9	16
72	Deformable wall effects on the detonation of combustible gas mixture in a thin-walled tube. International Journal of Hydrogen Energy, 2015, 40, 3006-3014.	7.1	24

#	Article	IF	CITATIONS
73	An Enhanced Particle Reseeding Algorithm for the Hybrid Particle Level Set Method in Compressible Flows. Journal of Scientific Computing, 2015, 65, 431-453.	2.3	12
74	Novel control of plasma expansion direction aimed at very low pressure laser-induced plasma spectroscopy. Optics Express, 2015, 23, 6336.	3.4	6
75	Towards clinical use of a laser-induced microjet system aimed at reliable and safe drug delivery. Journal of Biomedical Optics, 2014, 19, 058001.	2.6	22
76	Modeling of afterburning from the particle hydrodynamics of explosive product interface motion. Journal of Mechanical Science and Technology, 2014, 28, 4781-4787.	1.5	1
77	A high velocity impact experiment of micro-scale ice particles using laser-driven system. Journal of Applied Physics, 2014, 116, 173508.	2.5	7
78	Laser-induced microjet injection into preablated skin for more effective transdermal drug delivery. Journal of Biomedical Optics, 2014, 19, 118002.	2.6	24
79	Towards controlled flyer acceleration by a laser-driven mini flyer. Applied Physics A: Materials Science and Processing, 2014, 115, 971-978.	2.3	19
80	A reactive flow model for heavily aluminized cyclotrimethylene-trinitramine. Journal of Applied Physics, 2014, 116, .	2.5	31
81	Stand-off laser-induced breakdown spectroscopy of aluminum and geochemical reference materials at pressure below 1 torr. Spectrochimica Acta, Part B: Atomic Spectroscopy, 2014, 101, 335-341.	2.9	8
82	lgnition characteristics of laser-ablated aluminum at shock pressures up to 2 GPa. Journal of Applied Physics, 2014, 115, 013503.	2.5	1
83	Characterization of laser-induced ultrasound signal by reduced graphene oxide thickness and laser intensity. Applied Physics B: Lasers and Optics, 2013, 113, 389-393.	2.2	5
84	Analysis of melt-through process of 1.07 μm continuous wave high power laser irradiation on metal. Journal of Mechanical Science and Technology, 2013, 27, 1745-1752.	1.5	5
85	Laser-induced microjet: wavelength and pulse duration effects on bubble and jet generation for drug injection. Applied Physics B: Lasers and Optics, 2013, 113, 417-421.	2.2	11
86	Quantitative laser-induced breakdown spectroscopy of standard reference materials of various categories. Applied Physics B: Lasers and Optics, 2013, 113, 379-388.	2.2	12
87	A Smoothed Particle Hydrodynamics method with approximate Riemann solvers for simulation of strong explosions. Computers and Fluids, 2013, 88, 418-429.	2.5	24
88	Towards a two-dimensional laser induced breakdown spectroscopy mapping of liquefied petroleum gas and electrolytic oxy-hydrogen flames. Spectrochimica Acta, Part B: Atomic Spectroscopy, 2013, 88, 63-68.	2.9	21
89	Effect of multi-bend geometry on deflagration to detonation transition of a hydrocarbon-air mixture in tubes. International Journal of Hydrogen Energy, 2013, 38, 11446-11457.	7.1	21
90	A particle level-set based Eulerian method for multi-material detonation simulation of high explosive and metal confinements. Proceedings of the Combustion Institute, 2013, 34, 2025-2033.	3.9	31

#	Article	IF	CITATIONS
91	Melt-through characteristics in continuous beam irradiation of flying metal samples in flow speeds up to 85m/s. Optics and Laser Technology, 2013, 45, 250-255.	4.6	14
92	Understanding the anisotropic initiation sensitivity of shocked pentaerythritol tetranitrate single crystals. Applied Physics Letters, 2013, 103, 131912.	3.3	7
93	Er:YAG laser pulse for small-dose splashback-free microjet transdermal drug delivery. Optics Letters, 2012, 37, 3894.	3.3	46
94	Synthesis of Anatase Phase Titanium Dioxide Using High-Power Nd:YAG Laser Focused on Titanium Wire in Water. Materials Transactions, 2012, 53, 244-247.	1.2	2
95	Simulation of the vapor explosion of tin and aluminum oxide fragments in water. Combustion, Explosion and Shock Waves, 2012, 48, 455-464.	0.8	0
96	Spectroscopic detection of carbon particulates from a high speed jet stream with extended plasma visualization. Spectrochimica Acta, Part B: Atomic Spectroscopy, 2012, 74-75, 144-150.	2.9	1
97	Temperature-dependent absorptance of painted aluminum, stainless steel 304, and titanium for 1.07 μm and 10.6 μm laser beams. Optics and Lasers in Engineering, 2012, 50, 114-121.	3.8	44
98	Polarized reflectance of aluminum and nickel to 532, 355 and 266nm Nd:YAG laser beams for varying surface finish. Optics and Laser Technology, 2012, 44, 1823-1828.	4.6	11
99	A new particle method for simulating breakup of liquid jets. Journal of Computational Physics, 2012, 231, 1650-1674.	3.8	27
100	Laser-induced plasma peculiarity at low pressures from the elemental lifetime perspective. Optics Express, 2011, 19, 23097.	3.4	13
101	Simulation of the deflagration-to-detonation impact on a copper-based furnace injector. Combustion, Explosion and Shock Waves, 2011, 47, 457-463.	0.8	1
102	Dynamics of laser-induced bubble collapse visualized by time-resolved optical shadowgraph. Journal of Visualization, 2011, 14, 331-337.	1.8	32
103	Interaction of beam and coated metals at high power continuous irradiation. Optics and Lasers in Engineering, 2011, 49, 780-784.	3.8	5
104	INNOVATIVE DRUG INJECTION VIA LASER INDUCED PLASMA. , 2010, , .		0
105	Thrust enhancement via gel-type liquid confinement of laser ablation of solid metal propellant. Applied Physics A: Materials Science and Processing, 2010, 98, 147-151.	2.3	35
106	Performance analysis of a new biolistic gun using high power laser irradiation. Applied Physics A: Materials Science and Processing, 2010, 101, 417-422.	2.3	2
107	Metal and polymer melt jet formation by the high-power laser ablation. Applied Surface Science, 2010, 256, 2423-2427.	6.1	7
108	A laser based reusable microjet injector for transdermal drug delivery. Journal of Applied Physics, 2010. 107	2.5	39

#	Article	IF	CITATIONS
109	Predictive model of onset of pipe failure due to a detonation of hydrogen–air and hydrocarbon–air mixtures. International Journal of Hydrogen Energy, 2009, 34, 1613-1619.	7.1	10
110	Extended measurement of crater depths for aluminum and copper at high irradiances by nanosecond visible laser pulses. Applied Surface Science, 2008, 255, 2777-2781.	6.1	23
111	Shock compression of condensed matter using Eulerian multimaterial method: Applications to multidimensional shocks, deflagration, detonation, and laser ablation. Journal of Applied Physics, 2008, 103, 113507.	2.5	17
112	Shock compression of condensed matter using multimaterial reactive ghost fluid method. Journal of Mathematical Physics, 2008, 49, .	1.1	17
113	Ablation-induced explosion of metal using a high-power Nd:YAG laser. Journal of Applied Physics, 2008, 103, .	2.5	27
114	A STUDY OF PHASE EXPLOSION OF METAL USING HIGH POWER Nd:YAG LASER ABLATION. , 2008, , .		1